A potential red phosphor $ZnMoO_4$:Eu^{3+} for light-emitting diode application

Li-Ya Zhou *, Jian-She Wei, Fu-Zhong Gong, Jun-Li Huang, Ling-Hong Yi

School of Chemistry and Chemical Engineering, Guangxi University, Nanning 530004, People's Republic of China

A R T I C L E   I N F O

A B S T R A C T

Motivated by the need for new red phosphors for solid-state lighting applications Eu^{3+}-doped $ZnMoO_4$ was prepared by solid-state reaction and its photoluminescence properties were investigated. Compared with $Ca_{0.80}MoO_4$:$Eu_{0.20}^{3+}$, the obtained $Zn_{0.80}MoO_4$:$Eu_{0.20}^{3+}$ phosphor shows a stronger excitation band near 400 nm as well as enhanced red emissions (under 393 nm excitation). The strong red-emission lines at 616 nm correspond to the forced electric dipole $^5D_0 \rightarrow {}^7F_2$ transitions on Eu^{3+}. The chromaticity coordinates ($x = 0.63$, $y = 0.37$) are close to the standard of National Television Standard Committee (NTSC). The optical properties suggest that $Zn_{0.80}MoO_4$:$Eu_{0.20}^{3+}$ is an efficient red-emitting phosphor for LED applications.

1. Introduction

Since white light-emitting diodes (LEDs) can offer benefits in terms of high luminous efficiency, maintenance and environmental protection, they are called the next-generation solid-state light [1–5]. With the development of LED chip technology, the emission bands of LED chips shifted from blue light ($\sim$460 nm) to near UV range ($\sim$400 nm) and the near UV light can offer higher energy to pump the phosphor [6,7]. At present, the most widely used red phosphor for near UV InGaN-based LEDs is Y_2O_2S:Eu^{3+} [8], however, the efficiency of the Y_2O_2S:Eu^{3+} is much lower than that of the blue and green phosphors, and these sulfide-based phosphors are chemically unstable. Thus, special attention has been paid to phosphors with high absorption in the near UV spectral region. For high efficient phosphor in LEDs, the host must exhibit strong and broad absorption around 400 nm and the phosphor must show strong emission under $\sim$400 nm excitation and with the chromaticity coordinates near the standard of National Television Standard Committee (NTSC).

$ZnMoO_4$ belongs to the wolframite-type metal molybdates with triclinic symmetry, and has a high application potential in photoluminescence fields [9,10]. $ZnMoO_4$ is similar to $MgMoO_4$ in crystal structure and the $[MoO_4^{2-}]$ oxyanion complex is the principal constitutive element. The central Mo metal ion occupies three non-equivalent positions and is surrounded by four O^{2-} ions with approximately tetrahedral coordination. Considering the broad and intense charge transfer (CT) absorption bands in the near-UV and excellent thermal and chemical stability of such kind

of molybdates [4,11,12]; the $ZnMoO_4$ was chosen to be the host lattice in the Eu^{3+} ion-doped phosphors in this paper. The optical properties of the Eu^{3+} ion-doped into matrices are important to obtain a red-emitting phosphor with proper CIE chromaticity coordinates, because the lowest excited level ($^5D_0$) of the $4f^6$ configuration is situated below the $4f^55d$ configuration for Eu^{3+}, and it mainly shows sharp $^5D_0$–$^7F_2$ red-emission lines around 616 nm when Eu^{3+} ions occupy the lattice sites without centrosymmetry [13].

2. Experimental

2.1. Preparation of $ZnMoO_4$:Eu^{3+} phosphor

The phosphors $ZnMoO_4$:Eu^{3+} were prepared by solid-state reaction method at high temperature. ZnO (A.R. grade), $(NH_4)_6Mo_7O_{24} \cdot 4H_2O$ (A.R. grade) and Eu_2O_3 (99.99%) were used as reagents for sample preparations. Stoichiometric amount of starting materials were mixed homogeneously in an agate mortar and pre-calcined at 500 °C for 3 h, then calcined at 900 °C for 3 h.

2.2. Characterization of $ZnMoO_4$:Eu^{3+} phosphor

Powder X-ray diffraction (XRD, 40 kV and 200 mA, $CuK\alpha$ = 1.5406 Å Rigaku/Dmax—2500) was used to identify the structure of the final products. Analysis instrument of laser nanometer granularity (Zetasizer Nano S) was used to observe the distribution and size of the calcined particles. Near UV excitation and emission spectra were measured on an RF-5301PC fluorescence spectrophotometer use a Xe lamp as the excitation source. All the measurements were carried out at room temperature.

* Corresponding author. Fax: +86 771 3233718.
E-mail address: zhouliyatf@163.com (L.-Y. Zhou).

3. Results and discussion

3.1. XRD and size-distribution characterization

The powder XRD patterns of $Zn_{0.80}MoO_4:Eu_{0.20}^{3+}$ were shown in Fig. 1, and a and b were patterns for the samples calcined in air at 800 and 900 °C, respectively. The powder XRD patterns of the samples show that the phosphors are of single phase and consistent with JCPDS 72-1486 [$ZnMoO_4$], and the doped Eu^{3+} ion has little influence on the host structure. When the temperature increased from 800 to 900 °C, the widths of the peaks decrease and the intensity of the peaks become stronger because the crystal size grows, the relative intensities of the peaks change also because the crystals become larger. Once the temperature is up to 1000 °C, a melt form with $ZnMoO_4$ composition formed. From the XRD data, we can determine that

$ZnMoO_4$ has a triclinic structure (space group $P\bar{1}$ [2]) and its unit cell volume $V = 0.5138 \text{ nm}^3$. The corresponding unit cell volume of the sample in Fig. 1 is as follows: (a) $V = 0.5144 \text{ nm}^3$; (b) $V = 0.5146 \text{ nm}^3$. It is concluded that the doping of Eu^{3+} has enlarged the cell volume of the phosphor, which results from that the ionic radius of Eu^{3+} (0.107 nm) is slightly larger than that of Zn^{2+} (0.090 nm) and Mo^{6+} (0.041 nm) [14]. Due to the different valence states and difference of the ion sizes between Mo^{6+} and Eu^{3+}, Eu^{3+} is expected to occupy the Zn^{2+} site in this phosphor.

Fig. 2 shows the particle size distribution of $Zn_{0.80}MoO_4:Eu_{0.20}^{3+}$ calcined at 800 °C (a) and 900 °C (b), respectively. The particles show a narrow size distribution of about 0.9 μm after calcined at 800 °C. When the temperature increases from 800 to 900 °C, the size distribution of the phosphors increases obviously and the average diameter of the particles is about 1.2 μm, which is fit to fabricate the solid-lighting devices [15].
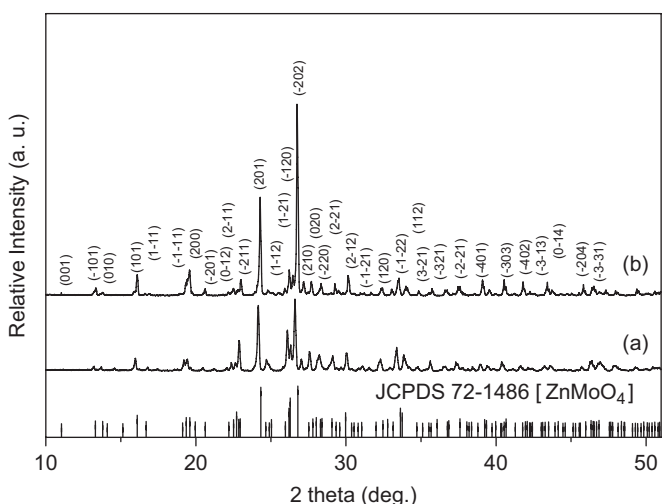
3.2. Photoluminescent properties

Fig. 3 shows the near UV excitation and emission spectra of the $Zn_{0.80}MoO_4:Eu_{0.20}^{3+}$ samples calcined at 800 and 900 °C, respectively. The broad excitation band from 220 to 350 nm is ascribed to the O–Mo CT transition and the sharp lines in the 360–500 nm range are intra-configurational $4f$–$4f$ transitions of Eu^{3+} in the host lattices, and the strong excitation band at ~393 and ~464 nm attributes to the $^7F_0 \rightarrow {}^5L_6$ and $^7F_0 \rightarrow {}^5D_2$ transitions of Eu^{3+}, respectively. Upon excitation with 393 nm UV irradiation, the emission spectra are described by the well-known $^5D_0 \rightarrow {}^7F_J$ ($J = 0$, 1, 2,…) emission lines of the Eu^{3+} ions with the strong emission for $J = 2$ at 616 nm, which allows that the Eu^{3+} occupies a center of asymmetry in the host lattice [16]. Other transitions from the ^5D_J excited levels to ^7F_J ground states in the 570–750 nm range are relatively weak. A ratio between the integrated intensity of these two transitions, I_{0-2}/I_{0-1}, is used in lanthanide-based systems as a probe of the cation local surroundings [17]. As shown in Fig. 3, the transition $^5D_0 \rightarrow {}^7F_2$ is much stronger than the transition $^5D_0 \rightarrow {}^7F_1$ and the ratio of I_{0-2}/I_{0-1}, is about 9.59 (800 °C) and 4.33 (900 °C),
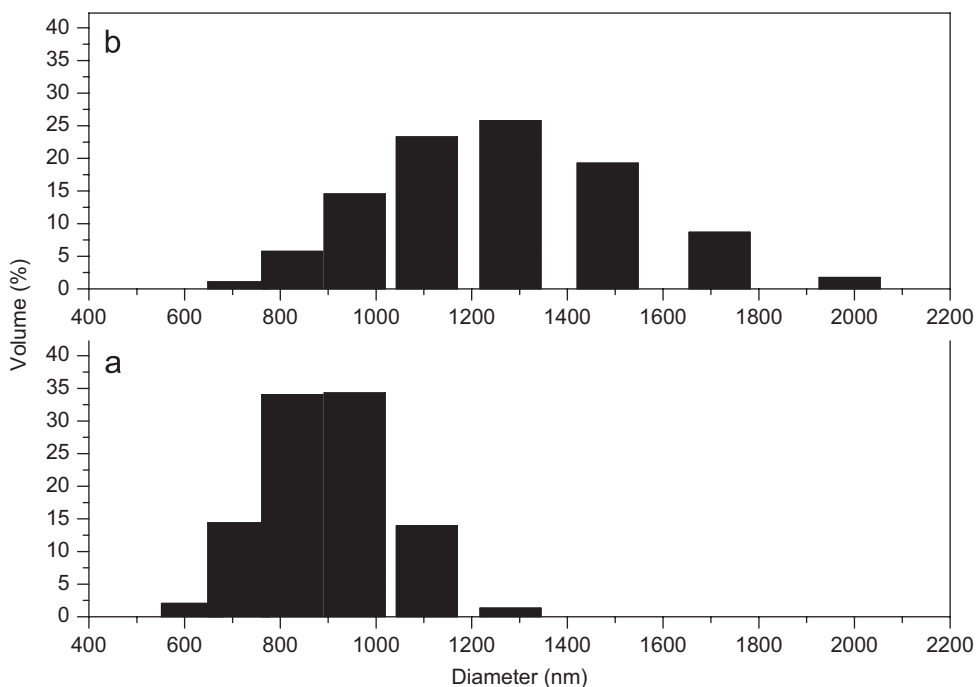

Fig. 1. XRD patterns of the $Zn_{0.80}MoO_4:Eu_{0.20}^{3+}$ phosphor calcined at (a) 800 °C and (b) 900 °C, respectively.

Fig. 2. Particle size distribution of $Zn_{0.80}MoO_4:Eu_{0.20}^{3+}$ phosphor calcined at (a) 800 °C and (b) 900 °C, respectively.
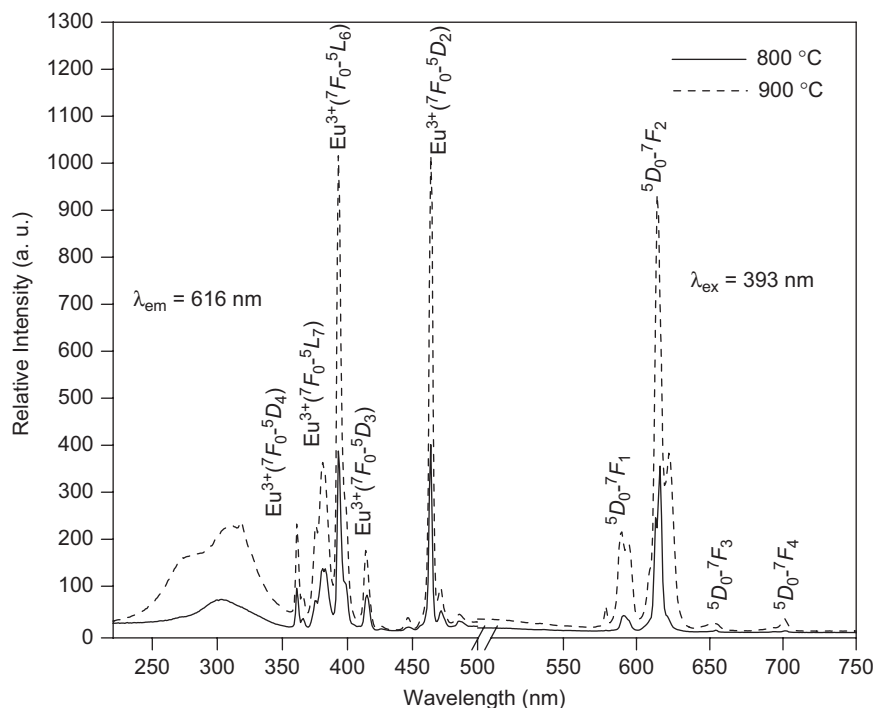
Fig. 3. UV excitation ($\lambda_{em} = 616$ nm) and emission ($\lambda_{ex} = 393$ nm) spectra of $Zn_{0.80}MoO_4:Eu_{0.20}^{3+}$ phosphor calcined at 800 and 900 °C, respectively.
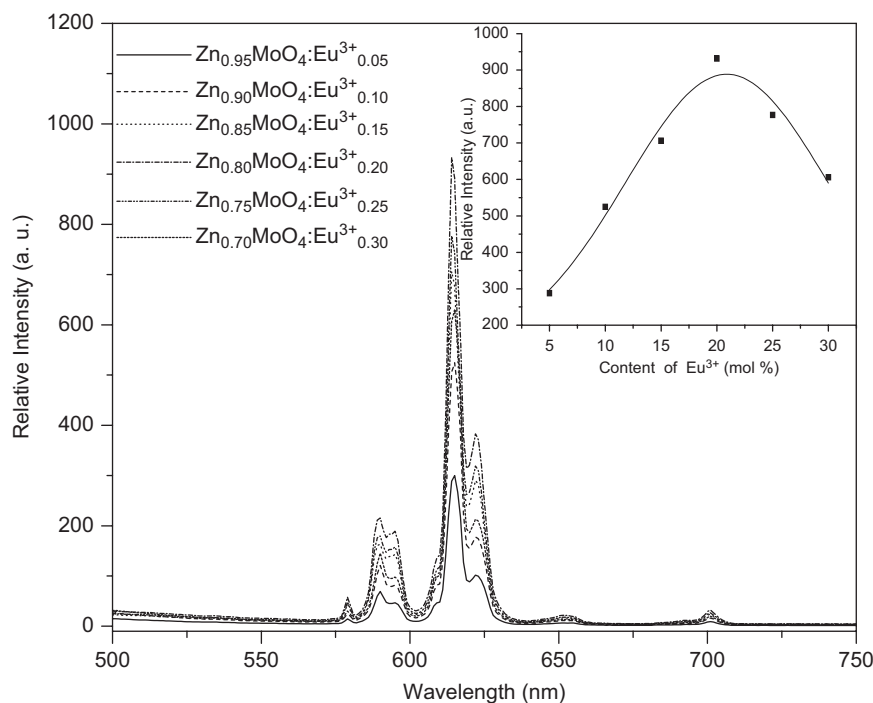

Fig. 4. Emission ($\lambda_{ex} = 393$ nm) spectra of $ZnMoO_4:Eu^{3+}$ phosphors with different Eu^{3+} doping ratios.

which suggests that the Eu^{3+} located in a distorted (or asymmetric) cation environment. This is favorable to improve the color purity of the red phosphor. The CIE chromaticity coordinates of the phosphor $Zn_{0.80}MoO_4:Eu_{0.20}^{3+}$ are calculated to be $x = 0.62$, $y = 0.38$ (800 °C) and $x = 0.63$, $y = 0.37$ (900 °C), which is close to the standard of NTSC ($x = 0.67$, $y = 0.33$). As the calcination temperature rises from 800 to 900 °C, the emission intensity increases due to the improvement of crystallinity [18].

The effect of the doped Eu^{3+} content in $Zn_{1-x}MoO_4:Eu_x^{3+}$ ($x = 0.05, 0.10, 0.15, 0.20, 0.25$ and 0.30) phosphors on the relative PL intensity at highest $^5D_0 \rightarrow {}^7F_2$ transition calcined at 900 °C is shown in Fig. 4. It can be seen that the luminescence intensity enhances with the increase of the Eu^{3+} doping ratio and reaches a maximum at 20 mol% of Eu^{3+}. When the Eu^{3+} doping ratio is higher above 20 mol%, the luminescence intensity reduces contrarily. This quenching process often attributes to energy migration
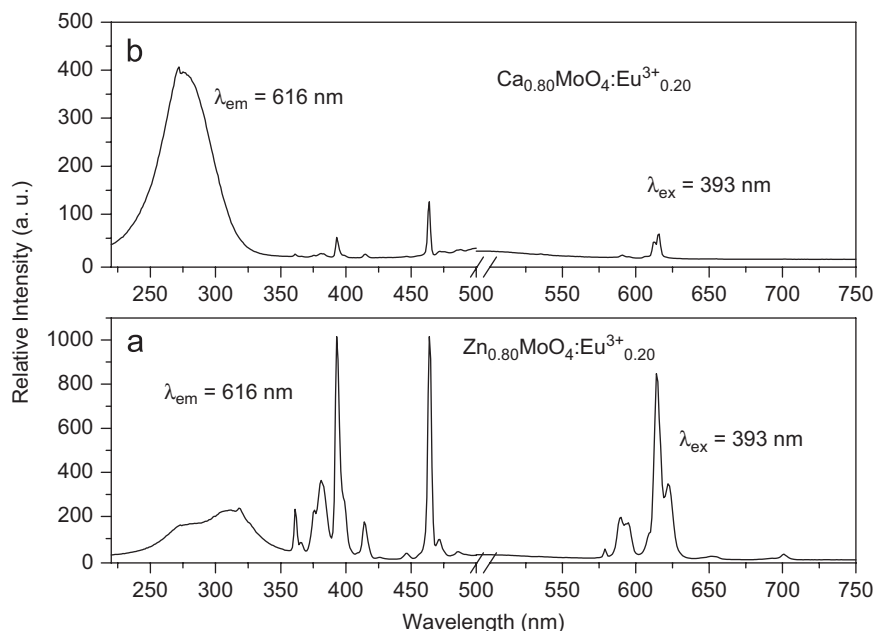
Fig. 5. UV excitation ($\lambda_{em} = 616$ nm) and emission ($\lambda_{ex} = 393$ nm) spectra of (a) $Zn_{0.80}MoO_4:Eu^{3+}_{0.20}$ and (b) $Ca_{0.80}MoO_4:Eu^{3+}_{0.20}$ phosphors.

among Eu^{3+} ions. Usually, an over-doping ratio perhaps brings quenching of the luminescence, for the doping concentration increase results in the enhancement of non-radiative relaxation between the neighboring Eu^{3+} ions. On the other hand, a low doping ratio gives a weak luminescence and it is unfavorable to luminescent applications. Therefore, the optimum mole concentration of Eu^{3+} in $Zn_{1-x}MoO_4:Eu_x^{3+}$ phosphors in this work is 20 mol%.

Fig. 5 shows the near UV excitation and emission spectra of the $Zn_{0.80}MoO_4:Eu^{3+}_{0.20}$ (a) and $Ca_{0.80}MoO_4:Eu^{3+}_{0.20}$ (b) by the solid-state reaction method calcined at 900 °C, respectively, and the optimum mole concentration of Eu^{3+} in $Ca_{1-x}MoO_4:Eu_x^{3+}$ phosphors is also 20 mol%. $CaMoO_4:Eu^{3+}$ is considered as a red potential phosphor that may substitute sulfide phosphors in white LEDs, because it shows not only desirable absorption in near UV region, but also excellent chemical and thermal stability, and when the excitation wavelength is 393 nm the emission intensity of $Y_2O_2S:0.05Eu^{3+}$ is only 37% of the $Ca_{0.80}MoO_4:Eu_{0.20}$ [6]. From Fig. 5(b), the dominant broad excitation band around 270 nm attributes to the O–Mo CT transition and the weak sharp lines in the 360–500 nm range are intra-configurational $4f$–$4f$ transitions of Eu^{3+} in the $CaMoO_4$ lattices. In the emission spectrum of $Ca_{0.80}MoO_4:Eu_{0.20}$, the main emission line is located at 616 nm, corresponding to the forced electric dipole transition ($^5D_0 \rightarrow {}^7F_2$) of Eu^{3+}. Comparing curve a with curve b, the O–Mo CT transition band in $Zn_{0.80}MoO_4:Eu^{3+}_{0.20}$ is located at around 330 nm, showing a slight longer-wavelength shifting, and a stronger excitation band around 400 nm is intra-configurational $4f$–$4f$ transitions of Eu^{3+}. Upon excitation with 393 nm UV irradiation, the emission intensity of $Ca_{0.80}MoO_4:Eu^{3+}_{0.20}$ is only 7% of the $Zn_{0.80}MoO_4:Eu^{3+}_{0.20}$ on the relative intensity of the highest line. The CIE chromaticity coordinates of the phosphor $Ca_{0.80}MoO_4:Eu_{0.20}$ are calculated to be $x = 0.62$ $y = 0.38$, which is close to the values ($x = 0.63$, $y = 0.37$) of $Zn_{0.80}MoO_4:Eu^{3+}_{0.20}$.

4. Conclusions

Eu^{3+}-doped $ZnMoO_4$ phosphors were prepared by solid-state reaction. Compared with the $Ca_{0.80}MoO_4:Eu^{3+}_{0.20}$ phosphor, the obtained $Zn_{0.80}MoO_4:Eu^{3+}_{0.20}$ phosphor shows a stronger excitation band around 400 nm and enhanced red emissions due to Eu^{3+} f–f transitions under 393 nm light excitation. The CIE chromaticity coordinates ($x = 0.63$, $y = 0.37$) of the phosphor are close to standard of NTSC. As the calcination temperature rises from 800 to 900 °C, the emission intensity increases due to the improvement of crystallinity, and the size distribution of the phosphors increases significantly and the average diameter of the particles is about 1.2 μm, which is fit to fabricate the solid-lighting devices. Upon excitation with near UV light, the phosphor showed strong red-emission lines at 616 nm correspond to the forced electric dipole $^5D_0 \rightarrow {}^7F_2$ transition of Eu^{3+}. All the results indicated that this red phosphor is a suitable candidate for the fabrication of near UV InGaN-based LEDs.

References

[1] J.S. Kim, P.E. Jeon, J.C. Choi, H.L. Park, S.I. Mho, G.C. Kim, Appl. Phys. Lett. 84 (2004) 2931–2933.
[2] Z.L. Wang, H.B. Liang, L.Y. Zhou, H. Wu, M.L. Gong, Q. Su, Chem. Phys. Lett. 412 (2005) 313–316.
[3] J.-H. Yum, S.-Y. Seo, S. Lee, Y.-E. Sung, J. Electron. Soc. 150 (2003) H47–H52.
[4] Y. Hu, W. Zhuang, H. Ye, D. Wang, S. Zhang, X. Huang, J. Alloy. Compds. 390 (2005) 226–229.
[5] S. Yan, J. Zhang, X. Zhang, S. Lu, X. Ren, Z. Nie, X. Wang, J. Phys. Chem. C 111 (2007) 13256–13260.
[6] Z. Ci, Y. Wang, J. Zhang, Y. Sun, Physica B 403 (2008) 670–674.
[7] Z.C. Wu, J.X. Shi, J. Wang, M.L. Gong, Q. Su, J. Solid State Chem. 179 (2006) 2356–2360.
[8] S. Neeraj, N. Kijima, A.K. Cheetham, Chem. Phys. Lett. 387 (2004) 2–6.
[9] R. Graser, E. Pitt, A. Scharmann, G. Zimmerer, Phys. Status Solidi—Basic Res. 69 (1975) 359–368.
[10] J.H. Ryu, S.-M. Koo, J.-W. Yoon, C.S. Lim, K.B. Shim, Mater. Lett. 60 (2006) 1702–1705.
[11] G. Blasse, Struct. Bond. 42 (1980) 1–3.

[12] V.B. Mikhailika, H. Krausa, D. Wahla, H. Ehrenbergb, M.S. Mykhaylyk, Nucl. Instrum. Meth. A 562 (2006) 513–516.
[13] Z. Wang, H. Liang, M. Gong, Q. Su, Opt. Mater. 29 (2007) 896–900.
[14] D. Lide (Editor-in-Chief), The CRC Handbook of Chemistry and Physics on CD-ROM, CRC Press, Boca Raton, FL, Version 2002, p. 12.
[15] R.P. Rao, J. Electrochem. Soc. 143 (1996) 189–197.
[16] S. Shionoya, W.M. Yen, Phosphor Handbook, CRC Press, Boca Raton, FL, 1999, p. 190.
[17] J.P. Rainho, L.D. Carlos, J. Rocha, J. Lumin. 87–89 (2000) 1083–1086.
[18] Y.H. Zhou, J. Lin, M. Yu, S.B. Wang, H.J. Zhang, Mater. Lett. 56 (2002) 628–636.